EFFECT OF THE WATER-WALL INTERACTION POTENTIALS ON THE PROPERTIES OF AQUEOUS SOLUTIONS CONFINED WITHIN A UNIFORMLY CHARGED NANO-CHANNEL

H. Hoang,[1] S. Kang[1] and Y. K. Suh[1]

Studies on the effect of the wall-ion, wall-water, water-ion and ion-ion interaction on properties of water and ions in nano-channels have been performed through the use of different kinds of ions or different models of potential energy between wall-ion or wall-water. On this paper, we address the effect of water-wall interaction potential on the properties of confined aqueous solution by using the molecular dynamics (MD) simulations. As the interaction potential energies between water and wall we employed the models of the Weeks-Chandler-Andersen (WCA) and Lennard-Jones (LJ). On the MD simulations, 680 water molecules and 20 ions are included between uniformly charged plates that are separated by 2.6 nm. The water molecules are modeled by using the rigid SPC/E model (simple point charge/Extended) and the ions by the charged Lennard-Jones particle model. We compared the results obtained by using WCA potential with those by LJ potential. We also compared the results (e.g. ion density and electro-static potential distributions) in each of the above cases with those provided by solving the Poisson-Boltzmann equation.

Key Words : Molecular Dynamics Simulation, Aqueous Solution, Hydrophobic Plate, WCA Potential, PPPM Methods

1. INTRODUCTION

The WCA potential is a special case of the Lennard-Jones potential but one is cut and shifted at the distance for which it is a minimum[1-4]. It is a purely repulsive potential since the WCA potential is shifted at the location of the energy minimum. For instance, the WCA potential corresponding to the 12-6 Lennard-Jones of two atoms, separated by r,isgivenas:

$$u(r)=\begin{cases}4\varepsilon\left(\left(\frac{\sigma}{r}\right)^{12}-\left(\frac{\sigma}{r}\right)^{6}\right)+\varepsilon & \text{if } r<2^{1/6}\sigma \\ 0 & \text{if } r>2^{1/6}\sigma\end{cases} \quad (1)$$

We therefore can examine the role of attractive part of the Lennard-Jones potential for the static and dynamic properties of the liquid by comparing the results obtained the Lennard-Jones potential with those by WCA potential.

Few studies have been reported recently[3-4], which the WCA potential is used to investigate the influence of the attractive part on the properties of the liquid. Travis et al (2000)[3] performed the molecular dynamics (MD) simulation on Poiseuille flow of Lennard-Jones fluid in narrow slit pores with use of different potentials for liquid-liquid, liquid-solid and solid-solid interactions(i.e. the Lennard-Jonesand WCA potential). They found that the liquid structures and velocity profiles are different in thes ecases. To investigate the effect of water-wall interaction potential on the properties of nano-confined water, Kumar et al (2007)[4] used various potential for liquid-solid interactions(the Lennard-Jones and WCA potential). They found that the properties of liquid are weakly dependent on the details of confining potential (potential between the wall and the fluid molecules) for the specific case of smooth walls. From these reports, we see that not that the attractive part strongly affect the properties of liquid in every case. However, no studies have been reported so far

1 동아대학교 기계공학부
* Corresponding author, E-mail: haicom_quanhau@yahoo.com

that consider the influence of the attractive part on the ions, water concentrations or polarization of water or diffusion of water, etc. for the aqueous solution confined in a uniformly charged hydrophobic channel.

In this paper, we used the MD method to study the effect of the water-wall interaction potential on the properties of aqueous solutions confined between uniformly charged nano-channel. We compared the results obtained by using WCA potential with those by LJ potential. We are also interested in comparison of our results with those provided by solving the PB equation.

Our paper is organized as following. In section 2, the detail of molecular models and MD simulations are presented. We provide the results of the MD simulations and discuss them in Section 3. Finally, the conclusions of our study are given in Section 4.

2. CONTINUUM MODEL OF ELECTRICAL DOUBLE LAYER

Under assumption of the continuum modeling, the EDL is described by solving the PB equation. The PB equation is combination of Poisson equation and Boltzmann distribution. The Poisson equation for the electric-static potential and a Boltzmann distribution for ion density are:

$$\varepsilon \nabla^2 \psi = -\rho_E \tag{2}$$

$$\rho_E = \sum_{i=1}^{N} \overline{z}_i e n_i \tag{3}$$

$$n_i = n_{\infty,i} \exp\left(-\frac{\overline{z}_i e \psi}{k_B T} \right) \tag{4}$$

The one-dimensional PB equation is:

$$\frac{d^2\psi}{dz^2} = -\frac{e}{\varepsilon} \sum_{i=1}^{N} \overline{z}_i n_{\infty,i} \exp\left(-\frac{\overline{z}_i e \psi(z)}{k_B T} \right) \tag{5}$$

where $\psi(z)$ is the local electrostatic potential, ρ_E is the local charge density, e the electron charge, ϵ the permittivity of the fluid in channel, T the medium temperature of fluid in the channel, k_B the Boltzmann constant, N the number of ion species, $n_i(z)$ the local number density, $n_{\infty,i}$ the number density at the channel center where the electrostatic potential is assumed to be zero and $\overline{z_i}$ is the valency.

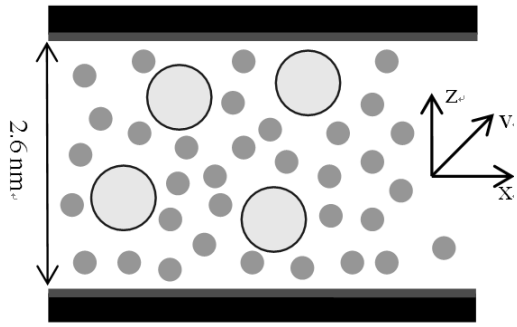

Fig. 1 Schematic of a nano-channel containing water molecules and ions. The inner surfaces of walls are uniformly charged. The darks dot indicate the water molecules and the shaded circles indicate ions Cl⁻

To be more convenient in the comparison of results of the continuum model and MD model, we used only one ion species which is mono-valent, which have charges opposite to wall charge to keep the system electro-neutral. Thus we can rewrite Eq. (5) as follows:

$$\frac{d^2\psi}{dz^2} = -\frac{e}{\varepsilon} \overline{z}_0 n_\infty \exp\left(-\frac{\overline{z}_0 e \psi(z)}{k_B T} \right) \tag{6}$$

Boundary conditions are:

$$\frac{d\psi}{dz} = 0 \quad \text{and} \quad \psi = 0 \quad \text{at } z = z_c \tag{7}$$

Integrating Eq. (6), we have the analytical solution:

$$\frac{d\psi}{dz} = \sqrt{\frac{2 k_B T n_\infty}{\varepsilon}} \left[\exp\left(-\frac{\overline{z}_0 e \psi}{k_B T} \right) - 1 \right]^{1/2} \tag{8}$$

$$\psi = \frac{k_B T}{\overline{z}_0 e} \ln\left[\cos^2\left(\frac{(z - z_c) e \sqrt{n_\infty \overline{z}_0^2}}{\sqrt{2 \varepsilon k_B T}} \right) \right] \tag{9}$$

Table 1 Parameters for the Lennard-Jones potential

Interaction	ε(kJ/mol)	σ(nm)
O-O	0.645	0.317
O-Wall	1.250	0.250
O-Cl	0.536	0.381
Cl-Cl	0.445	0.445
Cl-Wall	1.250	0.250

$$n_i = n_{\infty,i}\exp\left(-\frac{e\overline{z_0}\psi}{k_BT}\right) = n_{\infty,i}\frac{1}{\cos^2\left[\sqrt{\frac{n_\infty e^2\overline{z_0}^2}{2\varepsilon k_BT}}(z-z_c)\right]} \quad (10)$$

where $\overline{z_0}$ is the valency of ion, z_c is the coordinate of the channel center. In fact, Eq. (9) has been used by Freund and Kim et al[5-6]. In these equations, there is only one unknown value which is n_∞. To determine this unknown value, we used the following boundary condition:

$$\sigma_S = \varepsilon\frac{d\psi}{dz}(z = z_{wall}) \quad (11)$$

where σ_S is the surface charge density. Substituting Eq. (8) and Eq. (9) into Eq. (11), we derive the equation for the unknown value n_∞ as follow:

$$\sqrt{\frac{2n_\infty k_BT}{\varepsilon}}\left[\frac{1}{\cos^2\sqrt{\frac{n_\infty e^2\overline{z_0}^2(z-z_c)^2}{2\varepsilon k_BT}}}-1\right]^{1/2} = \frac{\sigma_s}{\varepsilon} \quad (12)$$

The unknown value n_∞ is determined by using the Newton-Rhapson method[17].

In the above computations we assumed the permittivity ϵ to be constant. In fact, the permittivity is varied with z coordinate. The permittivity of water in region adjacent to wall is largely different from those in the bulk. However, Freund[5] recently reported that the influence of permittivity variation in the channel on the ion distribution is less important compared to the ion-wall interaction. This implies that the use of constant or varied permittivity does not cause large difference in the result of ion distribution.

3. MOLECULAR-DYNAMIC SIMULATION

We performed the MD simulations of a system composed of 680 water molecules and 20 chloride ions confined between uniformly charged plates (Fig. 1). The SPC/E model (extended simple point charge) was used to describe the water molecules[8]. It is a three-site model, i. e. two sites for hydrogen atoms and one site for oxygen atom; all are located in a planar configuration. Both of charge and mass are coincidentally positioned at the sites of model. In the SPC/E model, O-H distance is fixed of 0.1nm and H-O-H angle equal to 109.47^0, point charges on the oxygen and hydrogen positions of -0.847e and +0.425e, respectively. The ions are modeled by the charged Lennard-Jones particle model. The interaction potential between the water molecule and the charged atom is constituted from (1) the Lennard-Jones potential of the oxygen atom and the atom, and (2) the electric potential of each site charge and the charge of the atom. To mimic the hydrophobic walls, we used the smooth walls that interact to atoms via the 9-3 Lennard-Jones potential as following[9]:

$$u_{L-J}(\Delta z) = 4\varepsilon\left(\left(\frac{\sigma}{\Delta z}\right)^9 - \left(\frac{\sigma}{\Delta z}\right)^3\right) \quad (13)$$

We computed the parameters for the 12-6 Lennard-Jones potential by using the Lorentz-Berthelot combination rule[16] and the same parameters used in previous studies for the 9-3 Lennard-Jones potential. All Lennard-Jones parameters are summarized in Table 1. The inner surface of each plate is uniformly charged of σ_s =0.156C/m^2.

To test the effect of the water-wall interaction potential on the static and dynamic properties of solution, we used the potential as Eq. (13), but truncated and shifted such that there is no attractive part in the potential, which is analogous to the WCA potential. In this way, understanding of the role of the attractive potential in determining the static and dynamic properties of the solution can be obtained. This WCA potential can be given as[4]:

$$u_{WCA}(\Delta z) = \begin{cases} 4\varepsilon\left(\left(\frac{\sigma}{\Delta z}\right)^9 - \left(\frac{\sigma}{\Delta z}\right)^3\right) + \frac{8}{3^{3/2}}\varepsilon & \text{if } \Delta z < 3^{1/6}\sigma \\ 0 & \text{if } \Delta z > 3^{1/6}\sigma \end{cases} \quad (14)$$

The motions of ions are described only by translation. The water molecules are modeled by rigid model; its motion is decomposed into two completely independent parts, translational motion of center of mass and rotation about the center of mass. In this study, we used a combination of quaternion coordinates with Euler angles to describe the motion of the rigid water molecules[13,16].

In MD simulations, we need to determine the motion

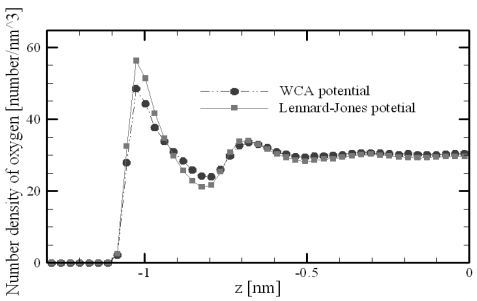

Fig. 2 The number density of oxygen across the channel

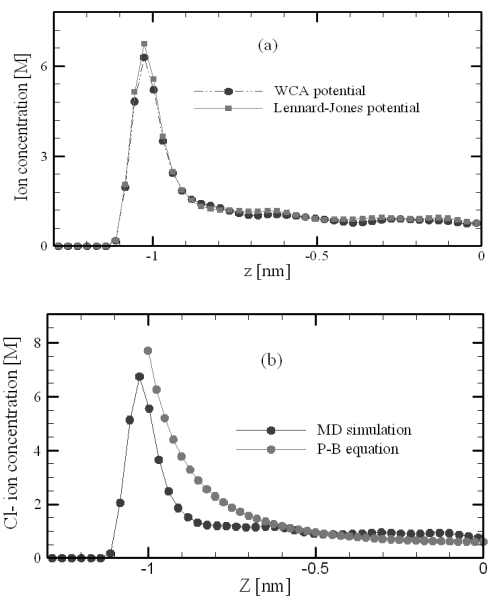

Fig. 3 The ion concentration across the channel. (a) The cases of the WCA and Lennard-Jones potentials. (b) Comparison of the PB and MD results in the case of the Lennard-Jones potential

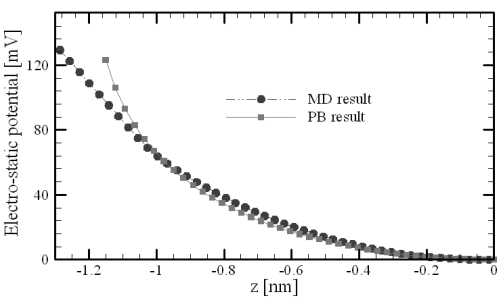

Fig. 4 The electro-static potential across the channel in the case of the Lennard-Jones potential

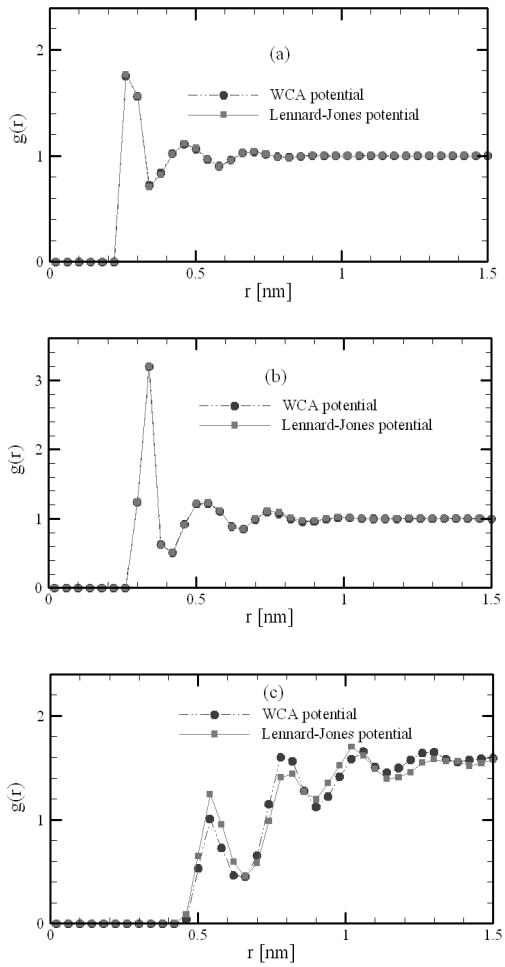

Fig. 5 The radial distribution functions in the x-y plane for both cases. (a) O-O RDF. (b) O-Ion RDF. (c) Ion-Ion RDF

equation of the molecules. The Newton's equation is applied to govern the translational and rotational motions of the molecules[13,16]. The potential energy of an atoms i, composed of the interaction potential between it and (1) other atoms in solution and (2) the walls, is given by:

$$V_i = \sum_{j \neq i} \varepsilon_{ij} \left(\left(\frac{\sigma_{ij}}{r_{ij}} \right)^{12} - \left(\frac{\sigma_{ij}}{r_{ij}} \right)^{6} \right) + \frac{q_i q_j}{r_{ij}} + \int_A \frac{q_i \sigma_s dxdy}{\sqrt{\left(r_i^x - x\right)^2 + \left(r_i^y - y\right)^2 + \left(r_i^z - z_{wall}\right)^2}} + V_i^{wall} \tag{15}$$

V_i^{wall} is the interaction potential between the atom ith and the wall without charge (i. e. Eq (13) or Eq. (14)).

The force exerting on each atom is of differentiation of Eq. (15), can be given as:

$$\mathbf{F}_i = \overrightarrow{grad}\ V_i \tag{16}$$

The EW3DC[10] (three dimensional Ewald-summation with the correction term) is most useful method to compute electric force for the systems with slab geometry. However, the EW3DC can not be directly applied for our case since there is no possible surface structure to obtain the positions of the surface charges (i. e. third term on right hand side in the Eq. (15)). This problem can be overcome by using the Yeh et al.'s modification[10] and the equivalent model of the parallel plate capacitor given by Yang et al[11]. We used the minimum-image criterion, cut-off and neighbor algorithm in order to effectively compute the Lennard-Jones and real-space forces with cutoff radius for Lennard-Jones force equal to 0.8 nm and 1.1 nm for the real-space force[13,16]. The PPPM[12] (particle-particle-particle-mesh) method is used for effectively computing the reciprocal space force for the non-surface charges. In this method, an FFT grid spacing of 0.1nm and a TSC (triangular shaped cloud, 2^{nd} order) for the charge distribution and the force interpolation were chosen.

The leap-frog Verlet algorithm was used to integrate the time differential equations with the numerical time step of 1.0 fs. To avoid the viscous heating, the Berendsen thermostat was used with the time constant 0.05 ps[13, 16]. The temperature T was calculated self consistently with three iterations.

Before starting the MD simulation, the initial positions, orientation, translational and rotational velocities of all the molecules have to be assigned[14]. The velocities were chosen randomly from a Gaussian distribution, which are corrected so that no overall linear momentum is produced; also magnitudes that should conforms to the required temperature 300K. We set up the rotational velocities for each water molecule in a similar way. We set their values randomly and then corrected so that there is no overall angular momentum, and conforming again to the required temperature at 300K[16].

We used the Euler angles combined with quaternion coordinates to describe the motion of rigid water molecules, so we must pay attention in setting the initial positions and orientations of molecules such that the intermolecular force and the torque should not be so large. To set-up the initial configuration, we performed two steps[14]. In the first step, all molecules were assigned with random positions and orientations. While keeping the orientations of the water molecules we performed the energy minimization to find the initial positions having small forces. The steepest descent method combined with the conjugate gradient method was applied in this energy minimization[17]. To implement the line minimization, we used the Brent method and parabolic interpolation with the spatial step size for the line search 0.01nm[17]. After this first step, we can get a configuration with small interaction force, but the interaction moment can be large. In order to reduce the magnitude of torque, we added damping terms to the Newton's equations. In our study, we chose that the damping coefficients for the force and the moment are 0.732 [N·ps/m] and 12.8 [ps^{-1}], respectively[14]. We set zero as the initial values for integration of the Newton's equations added the damping terms.

To reach the steady state, the system was simulated for the time duration 0.5 ns. After the system reached the steady state, we performed sampling every 10 fs in order to compute the average statistics for 1.5 ns for equilibrium MD simulations and 2.0 ns for non-equilibrium MD simulation except for the velocity autocorrelation functions (VACF). For the VACF, the sampling was also performed every 10 fs steps but only for 50 ps after 0.5 ns equilibration. The binning method was used to compute the values such as density, polarization, etc. across the channel. To remove the statistical noise, the noise reduction method is used in our post production[18].

4. RESULTS AND DISCUSSIONS

The equilibrium MD simulations have been performed by developing FORTRAN code. We present the numerical results as follows: In Sec. A, we provide the density of oxygen, ions and electro-static potential. In addition, we compare the MD results with those of P-B results. The radial distribution functions for every species pair are provided in Sec. B. The profiles of dipolar direction of water molecules across channel are computed in Sec. C. Finally, we compute the velocity autocorrelation function for both translational and rotational velocity and diffusion coefficient in Sec. D

4.1. DENSITY PROFILES OF OXYGEN, IONS AND ELECTRO-STATIC POTENTIAL DISTRIBUTION

The number density across the channel is defined as:

$$\rho(n) = \frac{1}{A\Delta z M} \sum_{j=1}^{M} \sum_{i=1}^{N} H_n\left(z_{i,j}\right) \tag{17}$$

$$H_n\left(z_{i,j}\right) = 1 \text{ if } (n-1)\Delta z \prec z_{i,j} \prec n\Delta z \tag{18}$$

where M is the numbers of samples and N is the number of particles.

Fig. 2 shows the number density of oxygen atom across the channel for both the WCA and Lennard-Jones potentials. We see that they are similar to each other such as form of profile, position of peaks and valleys, etc. On other word, the structure of water in direction perpendicular to surfaces is approximately same in both cases. However, the oxygen atoms in case of the Lennard-Jones case is more absorbed on the walls. This is to result from the influence of the attractive part of the force. We also performed the MD simulations in which the 9-pure repulsive potential (i. e. just the first term in the Lennard-Jones potential is considered) is employed for the interaction between atoms and the walls. The results will show in the presentation.

Fig. 3 shows the ion concentration across the channel for both the WCA and Lennard-Jones potentials. The distributions of ions in the channel are same in both cases. This implies that the influence of the attractive part of force on the distribution of the ions is much weak. In addition, we computed the ion concentration across the channel by solving the P-B equation [Eq. (5)] for comparison. The solution of the P-B equation is obtained by assuming that, in the Eq. (11), the position of the wall coincides with the position of the first peak of the ion concentration profile provided by the MD simulation and the permittivity of the water is constant in whole channel[5-7]. We see that the P-B solution and the MD result differ; especially, closer to the wall, more different between them. However, far away from the walls, they are approximately the same. This is because the assumptions of continuum model (e.g. the electrolyte ion could be regarded as point charge and the solvent could be treated as a structureless dielectric of constant permittivity) are invalid in the region adjacent to the walls.

Fig. 4 shows the electro-static potential across the channel. The P-B solution results from substituting n_∞, obtained as above, into Eq. (9). The MD electro-static potential, we obtained, is a solution of the Poisson equation, i. e. Eq. (2), with the ion density from the MD simulation and the assumption of the constant permittivity

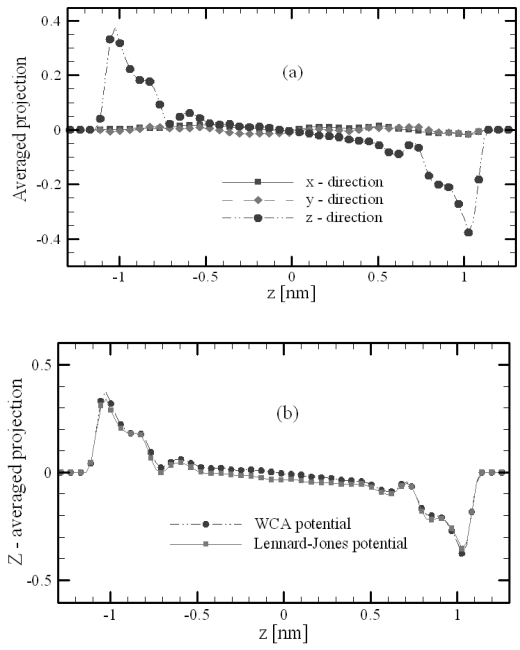

Fig. 6 The averaged projection of the water molecules across the channel. (a) The case of the Lennard-Jones potential. (b) Comparison of the z-component of the averaged projections in both cases

in whole channel. The P-B and MD solutions of course differ, since the ion densities across the channel are different from each other in both cases. We notice that P-B slope is steeper than the MD slope in the region close to the wall. This is contrary to those provided by Kim et al[6]. This contradiction is attributed to difference of the constant permittivity between our case and Kim et al.'s case[6]. We used the permittivity of the water to be constant in whole channel, while he used it, obtained the MD simulation, as varied in the channel. They found that the permittivity is strongly changed in the region adjacent to walls. We see that far away from the walls, the P-B and MD solutions are nearly the same.

4.2 Radial Distribution Functions

In the previous section, we addressed the effect of the attractive part of force on the structure of solvent and the distribution of the ion across the channel. In this section, we computed the radial distribution function (RDF), in the plane parallel to the wall surface, to understand further this effect on the structure of the solvent and the distribution of the ion. The RDF of a species X around to a Y species in the x-y plane is given as:

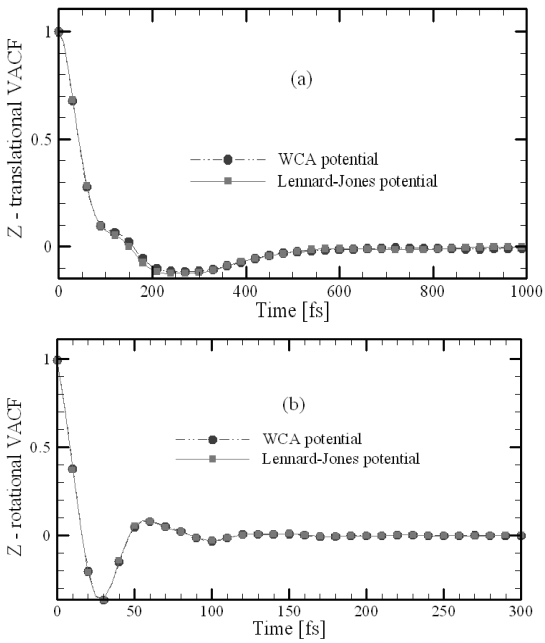

Fig. 7 Translational and rotational VACFs of the water molecules of the case of the Lennard-Jones potential in the first layer

$$g^{//}_{X-Y}(r)=\frac{1}{\rho_Y N_X}\sum_{i\in X}^{N_X}\sum_{j\in Y}^{N_Y}\delta(r-r_{ij})\left[\theta\left(|z_i-z_j|-\frac{\delta z}{2}\right)-\theta\left(|z_i-z_j|+\frac{\delta z}{2}\right)\right] \quad (19)$$

where ρ_Y is the density of the Y species, N_X and N_Y are number of the X and Y species respectively, r_{ij} is distance parallel to the x-y plane between molecules i and j, z_i is the z coordinate and $\delta(x)$ is the Dirac delta function. The Heaviside function $\Theta(x)$ restricts the sum to a pair of molecules located in the same slab of width δz. The physical interpretation of $g_{X-Y}''(r)$ is that $g_{X-Y}''(r)2\pi r dr\delta z$ is proportional to the probability of finding an X species molecule around to a Y species molecule in a slab of thickness δz at a distance r parallel to the walls from a randomly chosen molecule. In a bulk liquid, this would be identical to g(r), the standard RDF.

Fig. 5 shows the RDFs in various cases. We see that almost there is not difference between the WCA and Lennard-Jones results in two first cases. We hence expected that the last case have to be the same. However, the result has a bit difference in the last case, which is probably due to the statistical error. The statistical error in this case is slowly convergence, since the number of ion is a few. We can conclude that the effect of the attractive part of force on the structure of solvent and the distribution of the ion, in the plane parallel to the wall surface, is much weak.

4.3 Profiles of Polarization Density and Dipolar Direction of Water Molecules

In this section, we investigated the effect of the attractive part of force on the polarization of water by computing and comparing the averaged projection profiles of the water molecules across the channel in both cases. The computational domain is binned into the x-y plane along the z-direction. The averaged projection in the n^{th} bin with numbers of samples of M is defined as:

$$\chi(n)=\frac{1}{M}\sum_{j=1}^{M}\frac{\sum_{i=1}^{N}H_n(z_{i,j})\boldsymbol{\mu}_{water}}{\sum_{i=1}^{N}H_n(z_{i,j})|\mu_{water}|} \quad (20)$$

where, $\triangle z$ is width of the n^{th} bin, μ_{water} is the dipole moment vector of one water molecule. The physical interpretation of $\chi(n)$ is the averaged vector of the dipolar direction of the water molecule in the n^{th} bin.

Fig. 6(a) shows the averaged projection profiles across the channel in the case of the Lennard-Jones potential. In the x-, y- directions, the averaged projections are approximately equal to zero across the channel, which implies that the water molecules therefore are isotropically oriented in these directions. Otherwise, in the z-direction,

Table 2 The residence time of the water molecules in the first layer

	Residence time (fs)
WCA potential	650
Lennard-Jones potential	820

Table 3 The diffusion coefficient of the water molecules in the first layer. The unit diffusion coefficient is $10^{-9}m^2/s$

	D_{x-y}	D_z
WCA potential	2.93	2.28
Lennard-Jones potential	2.68	2.02

because of the interaction between the water molecules and the walls, the water molecules are preferably oriented, particularly in the region close to the walls. We notice that the position, at which the water molecules most preferably oriented, is to coincide to that of the first peak in the number density profile. The same observation is obtained in the previous studies. This phenomenon is related to the layering phenomenon.

Fig. 6(b) shows the z – component of the averaged projection profiles in both cases. We see that forms of profiles are nearly the same in whole channel. A small difference between them, it is attributed to the statistical error. We expected that there is a difference between them at the first peak of profiles. This figure shows that there is a small difference between them, but magnitude of derivation is less than that of the statistical error. Thus, this derivation is not clear to understand the effect of the attractive part of the force. We performed other MD simulation with the 9-pure repulsive part of the force considered. We will show its results in our presentation.

4.4 DYNAMIC PROPERTY

Up to now, we addressed the effect of the attractive part of the force on the static property of the solvent and the ion. We found that the static property of the solvent and the ion is weakly dependent on the attractive part, except for the water density in the region close to wall. In this region, the water molecules of the case of the Lennard-Jones potential are more absorbed on the walls. Thus, we expect that there is the difference between the WCA and Lennard-Jones results for the dynamic property in this region. In this section, we computed the VACFs of the translational and rotational motions, a residence time and the diffusion coefficient for the water molecule in the region close to the walls. The autocorrelation function of a quantity X can be defined as

$$c_X(t) = \langle X(t)X(0)\rangle = \frac{1}{M_0 N}\sum_{j=1}^{M_0}\sum_{i=1}^{N} X_i(t_j)X_i(t_j+t) \quad (21)$$

where M_0 is the number of time origins. If the quantity X is velocity then autocorrelation function is the so-called velocity autocorrelation function (VACF). The diffusion coefficient is related to the VACF by:

$$D = \frac{1}{d}\int_0^{\infty} c_v(\varsigma)d\varsigma \quad (22)$$

Fig. 7 shows the z directional normalized VACFs of the water molecules, in the region close to the walls, for the translational and rotational motions. The VACFs are normalized by the value at t = 0. We see that the traslational VACF decays lower than the rotational VACF, which is observed by Lyubartsev et al[15].

The residence time is the time duration before the VACF reaches to zero. In fact, we never obtain the exact zero value since the error occurs in the numerical and statistical computation. We hence defined the residence time as the time after when the normalized VACF is in range from -0.01 to +0.01. Table 2 shows the residence time of the water molecules in the region from -1.3 nm to -0.8 nm for both cases. The residence time, in the case of the Lennard-Jones potential, is longer than the other, which implies more the water molecules adsorbed on the walls. From the density profiles presented in the above section, we see that the water molecules are highly concentrated in the first layer in itself, for the case of the Lennard-Jones potential.

Table 3 shows the diffusion coefficients of the water molecules in the region from -1.3 nm to -0.8 nm for both cases, which are obtained by using the VACF [Eq. (22)]. We see that (1) the diffusion coefficient of the z-component is less than that of the x-y component in each case, and (2) the diffusion coefficient in the case of the Lennard-Jones potential is larger than that in the other. This is because of (1) the motions of the water molecules in the z – direction are strongly influenced by the walls, and (2) the water density in the case of the Lennard-Jones is larger.

5. CONCLUSIONS

By using the MD simulations, we have addressed the effect of the water-wall interaction potentials on the properties of aqueous solutions confined within a uniformly charged nano-channel. From the results above presented, we have some conclusions as following:

1. The static property of the solvent and ion is weakly dependent on the attractive part of the wall-water and water-ion interaction potentials. However, the water molecules are more absorbed on the walls in the case of Lennard-Potential.
2. By solving the P-B equation, we compared the MD with the P-B results. For the nano-scale system, the use of the continuum model can not predict the physical values (e. g. the ion concentration, the

electro-static potential) in the region close to the walls. However, far away from the channel surface, the physical values can be approximately obtained by solving the classical equation of the continuum model.

3. We computed the VACFs of the water molecules, in the region close to the walls, to understand the effect of the wall-water and water-ion interactions on the dynamic property of the water molecules. In this region, the water molecules in the case of the WCA potential are more mobilized and the wall-water and wall-ion interactions are to have effect on the dynamic property of the water.

ACKNOWLEDGMENTS

This work was supported by the Korea Science and Engineering Foundation (KOSEF) through the National Research Laboratory Program funded by the Ministry of Science and Technology (No. 2005-1091).

REFERENCES

[1] 2006, Heyes, D.M. and Okumura, H., "Equation of state and structural properties of the Weeks-Chandler-Andersen fluid," *Journal of chemical physics*, Vol.124, pp.164507(1-8).

[2] 2002, Tan, S.P., Adidharma, D. and Radosz, M., "Weeks-Chandler-Andersen Model for Solid-Liquid Equilibria in Lennard-Jones Systems," *Journal of physical chemistry B*, Vol.106, pp.7878-7881.

[3] 2000, Travis, K.P. and Gubbins, K.E., "Poiseuille flow of Lennard-Jones fluids in narrow slit pores," *Journal of chemical physics*, Vol.112, pp.1984-1994.

[4] 2007, Kumar, P., Starr, F.W., Buldyrev, S.V. and Stanley, H.E., "Effect of water-wall interaction potential on the properties of nanoconfined water," *Physical Review E*, Vol.75, pp.011202(1-8).

[5] 2001, Freund, J.B., "Electro-osmosis in a nanometer-scale channel studied by atomistic simulation," *Journal of chemical physics*, Vol.116, pp.2194-2200.

[6] 2006, Kim, D. and Darve, E., "Molecular dynamics simulation of electro-osmotic flow in rough wall nanochannels," *Physical Review E*, Vol.73, pp.051203 (1-12).

[7] 2002, Qiao, R. and Alura, N.R., "Ion concentrations and velocity profiles in nanochannel electroomostic flows," *Journal of chemical physics.*, Vol.118, pp.4692-4701.

[8] http://www.lsbu.ac.uk/water/models.html.

[9] 2005, Kumar, P., Buldyrev, S.V., Starr, F.W., Giovambattista, N. and Stanley, H.E., "Thermo-dynamics, structure, and dynamics of water confined between hydrophobic plates," *Physical Review E.*, Vol.72, pp.051503(1-12).

[10] 1999, Yeh, I.C. and Berkowitz, M.L., "Ewald summation for systems with slab geometry," *Journal of chemical physics*, Vol.111, pp.3155-3162.

[11] 2006, Yang, W., Jin, X. and Liao, Q., "Ewald summation for Uniformly Charged Surface," *Journal of Chemical Theory and Computation*, Vol.2, pp.1618-1623.

[12] 1998, Deserno, M. and Holm, C., "How to mesh up Ewald sums. II. An accurate error estimate for the particle–particle–particle-mesh algorithm," *Journal of chemical physics,* Vol.109, pp.7694-7701.

[13] 2002, Rapaport, D.C., *The art of molecular dynamics simulations*, Cambridge.

[14] 2008, Hoang, H., Kang, S. and Suh. Y.K., "Molecular-dynamic simulation on the equilibrium and dynamical properties of fluids in a nano-channel," *KSCFE (The Korean Society for Computational Fluid Engineering) Proceedings of Fall Conference, Seoul.*

[15] 1996, Lyubartsev, A.P. and Laaksonen, A., "Concentration Effects in Aqueous NaCl Solutions. A Molecular Dynamics Simulation," *Journal of Physical Chemistry*, Vol.100, pp.16410-16418.

[16] 1987, Allen, M.P. and Tildesley, D.J., *Computer Simulation of Liquids*, Clarendon Press, Oxford.

[17] 1992, Press, W.H., Teukolsky, S.A., Vetterling, W.T. and Flannery, B.P., *Numerical recipes in the Fortran*, 2nd ed., Cambridge.

[18] Help of MATLAB 7.0.